Theoretical and Applied Fracture Mechanics 95 (2018) 253–260

Contents lists available at ScienceDirect

Theoretical and Applied Fracture Mechanics

journal homepage: www.elsevier.com/locate/tafmec

# Strain evolution around corrosion pits under fatigue loading

Christopher Evans*, Rafael Leiva-Garcia, Robert Akid

*Corrosion Protection Centre, School of Materials, University of Manchester, Manchester M13 9PL, UK*

ARTICLE INFO

*Keywords:*
Fatigue
Pit-crack transition
Crack initiation
Digital image correlation
Full-field strain measurement

ABSTRACT

The effect of pit depth on the crack initiation life of the API-5L X65 steel was investigated by varying the depth of corrosion pits generated on fatigue specimens using a micro-electrochemical cell. Fatigue specimens were subjected to fatigue loading in air, during which time images of the surface around the pits were captured in-situ. Digital image correlation was employed to make full-field strain measurements at the mouth of corrosion pits from the images captured during testing. From these measurements, an average threshold strain value for crack initiation of 0.24 ± 0.06% was established. Whilst crack initiation life was observed to decrease with increasing pit depth, the threshold value was observed to be unaffected by pit depth. Images captured during the fatigue cycling were also used to calculate crack growth data. Crack growth rate was found to be influenced by pit depth for the first 150 µm of crack length, where greater pit depth facilitated higher crack growth rates due to an increased strain concentration around the deeper pits.

## 1. Introduction

Geometric surface discontinuities, such as notches, are known to initiate cracks in fewer fatigue cycles than an equivalent smooth surface, due to the presence of the notch acting as a stress concentrator. In the same way, corrosion pits, which have notch-like features, are also stress concentrators, and can act as precursors to cracking when subjected to fatigue loading. Once a pit grows to a critical shape and size, the associated stress concentration is enough for a crack to initiate [1–3].

As with the approach taken for notches, the severity of corrosion pits as stress concentrators can be approximated using the elastic stress concentration factor, $K_t$, However this is an elastic parameter, which does not take into account any localised plastic deformation that may occur due to localised stress exceeding the yield strength of the material. Cerit et al. performed numerical analyses to determine $K_t$ for a range of different pit sizes. They observed $K_t$ to be controlled by the aspect ratio of the pits (a/2c, where a is the pit depth and 2c is the pit width). Greater aspect ratio values produced greater values of $K_t$. The relationship between aspect ratio and $K_t$ is established through Eq. (1) [4].

$$K_t = \frac{\left[1 + 6.6\left(\frac{a}{2c}\right)\right]}{\left[1 + 2\left(\frac{a}{2c}\right)\right]} \quad (1)$$

A 3D elastic stress analysis in the same study found that the distribution of stress around the pit changed with aspect ratio. Lower aspect ratio pits were observed to have maximum stress near the bottom of the pit, whilst higher aspect ratios cause stress to localise near the mouth [4].

Further comprehensive studies of stress corrosion cracks initiating from pits were carried out by Turnbull et al., and Horner et al., using a combination of finite element analysis and experiments monitored using X-ray Computed Tomography (XCT) [5–7]. Finite Element Analysis (FEA) showed stress and strain to localise just below the pit mouth when the material was loaded to half of the 20% proof stress ($\sigma_{0.2}$). However, when the stress was increased to 90% $\sigma_{0.2}$, the stress concentration of the pit generated localised stress that surpassed the yield strength of the material. This resulted in the generation of plastic strain at the area of maximum stress; notably the pit mouth. The generation of strain and reduced constraint to plastic flow at the pit mouth caused the regions of high stress to be redistributed to the base of the pit [8]. This was confirmed using a purely elastic model, where under the same high stress levels, the stress and strain both remained at the pit mouth [5].

Although the study by Turnbull et al. was carried out under static tensile load, it is possible that a similar phenomenon will occur under fatigue loading. Turnbull et al. discuss the concept of dynamic strain, whereby the plastic strain at a pit increases as it grows [5]. This may explain why increasing pit depth has been observed to reduce fatigue crack initiation life in other studies [3,9,10].

Contrary to the observations of Turnbull et al., reports in the literature by other researchers have found cracks were be able to initiate at both the mouth [3,11,12] and the base [13–15] of pits. Of course the process of crack initiation is not simply a mechanical phenomenon;

* Corresponding author at: BAE Systems Submarines, Bridge Road, Barrow-in-Furness, Cumbria LA14 1AF, UK.
*E-mail address:* chris.evans9@baesystems.com (C. Evans).

https://doi.org/10.1016/j.tafmec.2018.02.015
Received 24 January 2018; Accepted 21 February 2018

interaction with the environment to promote crack initiation is also important [10,16]. Fang et al. stated that in near neutral pH conditions crack initiation from a pit occurred 3–4 orders of magnitude faster than fatigue cracks would initiate from the same pit in air [15]. The interaction between the mechanical and electrochemical aspects of crack initiation from pits is still not fully understood, therefore, the pit-crack transition still remains at the centre of current research.

In the power industry, turbines operate on a two-stage loading regime. When there is low demand for electricity the turbines are powered down and corrosion pits can initiate on turbine blades when the temperature drops and the environment becomes condensing, i.e., the system is wet. When demand for electricity increases the system is powered up and the temperature increases causing the environment to 'dry-out' and the corrosion pits cease to grow. In the 'on-load' stage the turbine is subject to fatigue loading and the pre-existing pits act as precursors to fatigue cracks, increasing the risk of reduced life of components.

To the knowledge of the authors, there have been no studies that have presented localised surface strain measurements taken from around a corrosion pit during the fatigue cycling events leading up to the pit-crack transition. The work carried out in this investigation aims to fill the gap in current knowledge by using digital image correlation (DIC) to measure strain around corrosion pits on specimens subjected to fatigue loading.

## 2. Experimental

Specimens were electrical discharge machined from API-5L X65 steel to the dimensions shown in Fig. 1. Following machining, specimen surfaces were ground using P80-P4000 grit paper. A micro-electrochemical cell (Fig. 2) was then used to create a pit of desired aspect ratio on the surface of the specimen (see Table 1 for pit dimensions, aspect ratio and stress concentration factor calculated using Eq. (1)). Pit geometry was measured using a Keyence VK-X200K 3D Confocal Laser Scanning Microscope.

Following pit generation, the specimen surfaces were polished to a 0.25 μm finish using diamond paste, and etched in 2% nital solution to create a pattern for the DIC (Fig. 3). A Micro-Measurements WK-06-125AD-350 strain gauge was then attached to the back of each specimen (directly behind the pit) using P-2 Strain Gauge Adhesive by TML. The adhesive was then cured at 50 °C for 1 h.

Images for DIC were captured using a Zeiss V12 stereomicroscope modified for use with a pair of La Vision Imager Elite™ CCD cameras, mounted adjacent to an Instron Electropuls E10000 dynamic load frame (10 kN capacity) (Fig. 4). The objective was a Zeiss Acromat x.63 (working distance, 100 mm). A magnification of 32 × was employed for imaging, which resulted in a single pixel size of approximately 1 μm. Illumination was provided by a Zeiss EasyLED ring light system.

Fatigue cycling was performed with a stress range (Δσ) of 450 MPa, a cyclic frequency of 15 Hz and a stress ratio of R = 0.1. A 5 V trigger signal sent via a connection between the load frame controller unit and the trigger unit of the DIC system enabled the automation of in-situ image acquisition during testing.

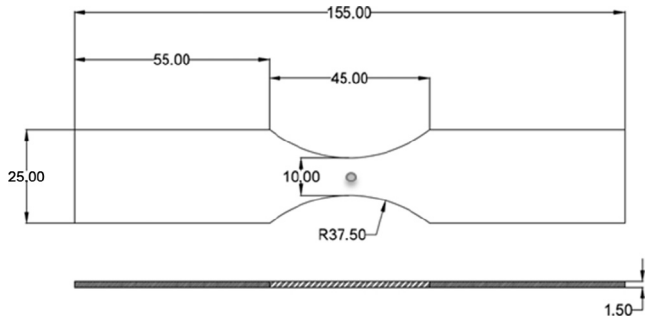


**Fig. 1.** Schematic of fatigue specimen (units of length = mm). Pit location is shown in the centre of the gauge section.

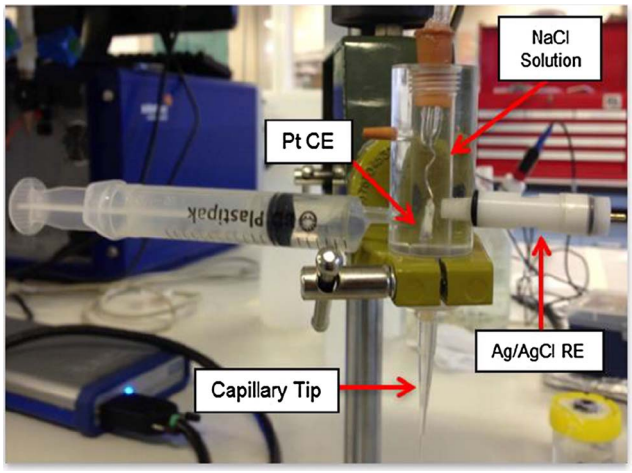


**Fig. 2.** The micro-electrochemical cell used to generate artificial corrosion pits on fatigue specimens. CE, counter electrode; RE, reference electrode.

**Table 1**
Pit geometries used for pitted specimens.

| Specimen | Pit geometry group | Average depth (μm) | Average width (μm) | Aspect ratio | Stress Concentration factor |
|---|---|---|---|---|---|
| 1 | 190 μm | 194 ± 1 | 632 ± 2 | 0.31 | 1.87 |
| 2 | | 191 ± 2 | 627 ± 4 | 0.30 | 1.87 |
| 3 | 270 μm | 255 ± 1 | 682 ± 11 | 0.37 | 1.98 |
| 4 | | 249 ± 1 | 681 ± 3 | 0.36 | 1.97 |
| 5 | 380 μm | 375 ± 2 | 795 ± 10 | 0.47 | 2.12 |
| 6 | | 407 ± 1 | 807 ± 3 | 0.50 | 2.15 |
| 7 | | 400 ± 6 | 787 ± 5 | 0.51 | 2.16 |
| 8 | 440 μm | 422 ± 3 | 781 ± 4 | 0.54 | 2.19 |
| 9 | | 460 ± 3 | 793 ± 4 | 0.58 | 2.24 |
| 10 | | 458 ± 3 | 823 ± 3 | 0.55 | 2.21 |

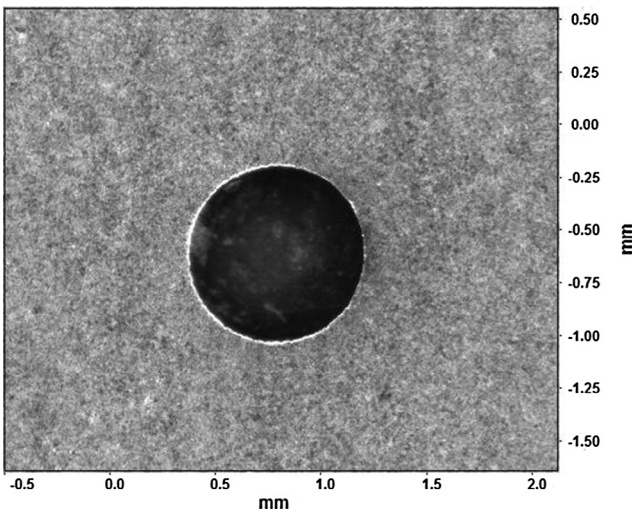


**Fig. 3.** Etched speckle pattern captured using the DIC stereomicroscope system.

Images were captured from the specimen in strain control at the same applied strain value in order to capture changes in plastic strain. At the start of each test sequence a reference image was captured at the strain value ($\varepsilon_{max}$) corresponding to the maximum load. The sequence then entered a programmed loop where the specimen was cycled in